# Chapter 6

# Eddy Viscosity and Hyperviscosity

Models for the subgrid-scale dissipation in numerical simulations of turbulence have long been necessary in the study of atmospheric and oceanographic turbulence, for which the direct numerical simulation of the full range of scales is infeasible. 'Large Eddy Simulations' (LES) (Galperin and Orszag 1993) evolve the largest scales of a problem and model the average interaction with the unresolved small scales through dissipative terms called eddy viscosity. Our goal is to apply these techniques to simulations of drift-wave turbulence in tokamaks. This preliminary study tests some basic dissipative terms in a simple 2D drift-wave model. By restricting the problem to two dimensions, a large number of simulations can be performed with sufficient time histories for the statistics necessary to compute the eddy viscosity. In Chapter 7 extensions to three dimensions are discussed and applied to gyrofluid turbulence simulations.

When it is computationally impossible to resolve the dissipation scales in homogeneous isotropic turbulence, the standard tool used in numerical simulations is hyperviscosity, a damping rate of the form $M|\mathbf{k}|^p$ where the power $p$ is larger than 2; $p = 2$ gives ordinary viscosity. Hyperviscosity introduces an artificial dissipation range into the problem that is narrower than the usual dissipation range and therefore requires less resolution. The choice of power and magnitude is somewhat arbitrary. Numerical studies of 2D Navier–Stokes turbulence have found that a moderately high power ($p = 8$ or $p = 16$) allows the hyperviscosity to effectively remove energy from small scales with a minimum of unphysical dissipation at the large scales (Basdevant and Sadourny 1983). While the dissipation range introduced by hyperviscosity acts as a model for the true dissipation range, the damping provided by hyperviscosity has not been systematically compared with the nonlinear transfer rates to unresolved scales.

Eddy viscosities attempt to model the sink of energy at small scales by introducing dissipation into the resolved scales. The nonlinear viscosity of Smagorinsky (1963), for example, is a simple model with a long history of applications in fluid turbulence. The damping given by the Smagorinsky viscosity is proportional to $|\mathbf{k}|^2$, which is rigorously correct only in the limit where the separation of scales between resolved and unresolved modes is asymptotically large. When there is significant transfer of energy that is local in $k$ space, as in Navier–Stokes turbulence, the contribution to the eddy viscosity from local transfer to unresolved modes near the cutoff is poorly represented by a $k^2$ damping rate (Kraichnan 1976). This theoretical eddy viscosity has been tested for the inverse cascade range in large eddy simulations of 2D Navier–Stokes turbulence (Chekhlov 1995).

The ideas of hyperviscosity and eddy viscosity are combined here to create a nonlinear filter for use in simulations of drift-wave turbulence. Theoretical predictions of the nonlinear transfer do not yet exist for comprehensive models of drift-wave turbulence. For simple drift-wave models, predictions of the nonlinear transfer from closure theories have only been made very recently (Hu et al. 1997). Therefore, the approach taken here is to choose the form of the hyperviscosity model by comparison with direct numerical simulations. The eddy viscosity is calculated for a given set of parameters and resolution from a higher-resolution simulation by calculating the transfer from modes that are contained in the low-resolution simulation to all other modes. The eddy viscosity was calculated in this fashion for a wide range of parameters and various resolutions. The hyperviscosity was fit to the calculated damping rate by adjusting the power and magnitude. The power $p$ and magnitude $M$ were then parameterized as functions of the resolved modes based on insights from Kraichnan's eddy viscosity for the 2D enstrophy range.

The resulting parameterized hyperviscosity has several advantages over traditional approaches. The choice of power and magnitude are calculated from functions of the resolved scales, eliminating what are arguably free parameters in the standard application of hyperviscosity. The damping rate comes closer to modeling the actual eddy damping rate than do eddy viscosities like Smagorinsky's that have damping rates proportional to $k^2$. For problems of interest, the actual eddy damping rate has not been predicted theoretically and can only be calculated from high resolution simulations. This method is straightforward to implement in spectral simulations of homogeneous turbulence, where $k$-dependent damping rates are trivial to incorporate.

The parameterization is based on the general physical processes of nonlinear advection and 2D enstrophy cascade. This model should therefore be useful for more general drift-wave calculations that resolve the main energy injection scales and are using this hyperviscosity only to reduce the resolution needed for modes at scales smaller than the injection scales. This model may also be useful for passive-scalar advection problems. Situations with inverse cascade and significant energy production at unresolved scales, such as may be found in magneto-hydrodynamic turbulence or 2D Navier–Stokes turbulence, result in negative eddy viscosities and are therefore clearly beyond the scope of this model, but have been studied with other models (Chekhlov 1995).

## 6.1 Large Eddy Simulation

The model equation (5.9) can be written symbolically as

$$\frac{\partial}{\partial \tau}\psi = N(\psi) + L\psi, \tag{6.1}$$

where $L$ is a linear operator and $N$ is the quadratic nonlinearity defined by Eq. (5.11). Numerical simulations cannot follow the detailed behavior of the continuous field $\psi$. Pseudospectral simulations on a periodic box of size $l \times l$ with a finite number of modes are considered. The resolved modes (those that are evolved in a simulation) can be defined through a filter function, $f \to \overline{f}$, such that in Fourier space

$$\overline{f}_{\mathbf{k}} = G_{\mathbf{k}} f_{\mathbf{k}}, \tag{6.2}$$

where $G_{\mathbf{k}} = 1$ for $|k_x| < k_x^c$ and $|k_y| < k_y^c$, and $G_{\mathbf{k}} = 0$ otherwise. (The boundary wave numbers $k_x^c$ and $k_y^c$ are called the cutoff wave numbers. For theoretical studies of isotropic turbulence, a spherical region in $k$ space, $|\mathbf{k}| \le k_c$, is typically used.) Fields such as the potential $\psi$ can then be decomposed into a resolved part $\overline{\psi}$ and a subgrid contribution $\psi^s = \psi - \overline{\psi}$. The filtered evolution equation can be written as

$$\frac{\partial}{\partial \tau}\overline{\psi} = \overline{N(\overline{\psi})} + N^s + L\overline{\psi}, \tag{6.3}$$

where the subgrid contribution to the nonlinear term is defined by

$$N^s = \overline{N(\psi)} - \overline{N(\overline{\psi})}. \tag{6.4}$$

Given the resolved field $\overline{\psi}$, pseudospectral evaluation of the nonlinear term gives precisely $\overline{N(\overline{\psi})}$, so the only term in the evolution equation (6.3) that is not calculated in a simulation of the resolved field is the subgrid contribution $N^s$.

The field of Large Eddy Simulation is concerned with deriving approximate models for the effect of the subgrid term $N^s$ that can expressed in terms of the resolved field $\overline{\psi}$. Traditionally it is argued that the average contribution of the subgrid term $N^s$ can be viewed as an eddy viscosity, draining energy from the resolved scales.

If there were a true separation of scales and the subgrid field $\psi^s$ had asymptotically short wavelengths and short time scales compared to the resolved field $\overline{\psi}$, then the subgrid term would truly act like a viscosity (Kraichnan 1987). Upon averaging over a time that is short for the resolved modes but long compared to the turnover time for the subgrid modes, we would find that $\langle N^s \rangle = \nu_{\text{eddy}} \boldsymbol{\nabla}^2 \overline{\psi}$, where the eddy viscosity $\nu_{\text{eddy}}$ is a function of the statistics of the small scales. In reality, however, the length and time scales of the subgrid modes are nearly identical to those of barely resolved modes.

Various approaches to estimating the subgrid contribution have been proposed. We will examine two simple estimates: a $k$-space-dependent eddy viscosity, and the eddy viscosity of Smagorinsky (1963). In numerical simulations, application of these approaches corresponds to introducing a simple dissipative term [$N^s_{\mathbf{k}} \approx \nu_k k^2 \psi_{\mathbf{k}}$ or $N^s \approx \boldsymbol{\nabla} \cdot \nu(\mathbf{x}) \boldsymbol{\nabla} \psi$ respectively] where the damping [$\nu_k$ or $\nu(\mathbf{x})$] is predicted either theoretically or empirically as a function of the resolved scales. Several authors have pointed out that in a turbulent state subgrid scales do not act in a purely dissipative fashion and that a more complete model would contain terms to simulate noise and backscatter of energy from the subgrid scales (Rose 1977). Simple damping terms, however, are extremely efficient to calculate. It is not clear which approach, adding higher-order terms to the subgrid model or increasing grid resolution with a simple subgrid model, is more efficient at improving the statistics of the long-wavelength modes for a given increase in computational complexity. For the current study, simple dissipative terms are considered.

### 6.1.1 Smagorinsky Eddy Viscosity

A traditional view of eddy viscosity is that the short-wavelength modes act in some sense like a thermal noise on the resolved scales and hence serve to enhance the regular viscosity. Estimating the subgrid contribution by a spatially varying eddy viscosity yields

$$N^s \approx \boldsymbol{\nabla} \cdot \nu_{\text{eddy}}(\mathbf{x}) \boldsymbol{\nabla} \psi(\mathbf{x}). \tag{6.5}$$

Smagorinsky (1963) gave heuristic arguments for the scaling of this eddy viscosity in the context of simulations of quasi-geostrophic turbulence; he concluded that

$$\nu_{\text{eddy}}(\mathbf{x}) = (C_s d)^2 S(\mathbf{x}, t), \tag{6.6}$$

where $C_s$ is a non-dimensional constant, $d$ is an estimate of the subgrid length scale, and $S(\mathbf{x}, t)$ is the local strain rate of the velocity field defined by

$$S(\mathbf{x}, t) = \sqrt{\left(\frac{\partial V_x}{\partial x}\right)^2 + \left(\frac{\partial V_y}{\partial y}\right)^2 + \frac{1}{2}\left(\frac{\partial V_x}{\partial y} + \frac{\partial V_y}{\partial x}\right)^2}. \tag{6.7}$$

Note that $S = 0$ for rigid rotation as well as for uniform flows.

The Smagorinsky model has been applied in computations of flows far outside the realm of its original derivation, with success in many cases. This model was used in simulations in this study for the purpose of comparison, to illustrate the behavior of the standard eddy viscosity with $k^2$ damping. Different choices of length scale and constant have been found to give optimal results in different situations in fluid turbulence. We therefore arbitrarily set $d$ to the physical-space grid spacing, and used $C_s = 0.1$ based on initial tests for one choice of parameters with moderate resolution.

### 6.1.2 Kraichnan's Eddy Viscosity

One approach to defining a damping term originating from the subgrid modes is by comparing the nonlinear transfer term with the viscous term in a two-point closure theory (Kraichnan 1976). By splitting the modes into resolved modes and subgrid modes, the quadratic invariant evolution equation (5.16) can be written as

$$\left(\frac{\partial}{\partial\tau} - 2\gamma_{\mathbf{k}}\right)\Omega_{\mathbf{k}} = T^r_{\mathbf{k}} + T^s_{\mathbf{k}}, \tag{6.8}$$

where the transfer defined in Eq. (5.17) has been decomposed into a resolved piece $T^r_{\mathbf{k}}$ and the subgrid piece $T^s_{\mathbf{k}}$. In the context of this equation, the analog to Kraichnan's *effective eddy viscosity* would be defined as

$$\nu_{\mathrm{eddy}}(\mathbf{k}) = \frac{-\langle T^s_{\mathbf{k}}\rangle}{2k^2\langle\Omega_{\mathbf{k}}\rangle}, \tag{6.9}$$

for some appropriately defined ensemble average. The motivation for this definition of an eddy viscosity comes from introducing a damping term of the form $-\nu_{\mathrm{eddy}}(\mathbf{k})k^2\psi_{\mathbf{k}}$ on the right-hand side of the primitive equation (5.10). This damping term would introduce the term $-\langle T^s_{\mathbf{k}}\rangle\Omega_{\mathbf{k}}/\langle\Omega_{\mathbf{k}}\rangle$ to the right-hand side of Eq. (6.8) above, which, on average, will balance the subgrid transfer term $T^s_{\mathbf{k}}$.

Kraichnan derives predictions of this eddy viscosity (Kraichnan 1976) in 2D and 3D Navier-Stokes inertial ranges using the Test Field Model (Kraichnan 1971). While plasma turbulence is not expected to exhibit inertial-range behavior, there are several generic conclusions about eddy viscosity worth noting. The primary discovery was that the eddy viscosity does not give a damping rate proportional to $k^2$ that is traditionally associated with an eddy viscosity. The eddy viscosity does asymptote to a constant value at long wavelengths. This constant, however, is negative for 2D turbulence. The major contribution to the subgrid energy transfer comes from coherent straining of the short-wavelength modes by long-wavelength velocity shear, which causes the eddy viscosity to become large and positive near the high-wave-number cutoff $k_c$. The simulations considered here correspond most closely to the 2D case where the cutoff $k_c$ lies in the enstrophy range. For this case, the significant positive contribution to the eddy viscosity lies in a region near the cutoff wave number $k_c$ of width $k_0$, where the straining field is dominated by wave numbers of size $k_0$ and smaller. The shape of the eddy-viscosity function in this region depends on the nature of the spectrum at long wavelengths. For an artificial spectrum that allowed for a simpler calculation, the eddy viscosity in the near-cutoff region was found to be

$$\nu_{\mathrm{eddy}}(k) \approx (\theta k_c k_0)^{-1} f\left(\frac{k_c - k}{k_0}\right) \qquad [(k_c - k) \ll k_c], \tag{6.10}$$

where $\theta$ is the eddy circulation time of the long wavelengths. See Eq. (6.5) of Kraichnan (1976).

### 6.1.3 Numerical Eddy Viscosity

In the original work on this eddy viscosity (Kraichnan 1976), the subgrid transfer $\langle T^s \rangle$ was viewed as a theoretically derived quantity containing contributions from all three-mode couplings that cross the cutoff in $k$ space. The standard approach to calculating eddy viscosity in numerical simulations (Maltrud and Vallis 1993; Chekhlov et al. 1994) defines the subgrid transfer based on the subgrid contribution to the nonlinear term as defined in Eq. (6.4). For our model the subgrid transfer is defined by

$$T_{\mathbf{k}}^s = \left[(1+|\mathbf{k}|^2)^2 + {\delta_0}^2 {k_y}^2\right] 2\mathrm{Re}(\psi_{\mathbf{k}}^* N_{\mathbf{k}}^s). \tag{6.11}$$

Substituting this definition for $T^s$ into the definition of eddy viscosity in Eq. (6.9) yields

$$\nu_{\mathrm{eddy}}(\mathbf{k}) = -\frac{\mathrm{Re}\Big(\langle \psi_{\mathbf{k}}^* N_{\mathbf{k}}^s \rangle\Big)}{k^2 \left\langle |\psi_{\mathbf{k}}|^2 \right\rangle}. \tag{6.12}$$

With this definition, the eddy-viscosity approximation for the subgrid term,

$$N_{\mathbf{k}}^s \approx -\nu_{\mathrm{eddy}}(\mathbf{k}) k^2 \psi_{\mathbf{k}}, \tag{6.13}$$

can be viewed as the linear (in $\psi_{\mathbf{k}}$) approximation that minimizes the mean-squared residual error.

To calculate the eddy viscosity for a given low-resolution simulation with cutoff wave number $k_c$, a simulation is performed at much higher resolution containing a large number of higher-$k$ modes ($|\mathbf{k}| > k_c$) along with all the modes resolved by the low-resolution simulation. The 'unresolved' component of the nonlinear term $N^s$ defined in Eq. (6.4), is calculated for the low-resolution simulation from modes resolved in the higher-resolution simulation. Calculating the eddy viscosity from high-resolution simulations to apply to low-resolution simulations cannot by itself reduce the computational cost of a particular problem since presumably the high-resolution simulations yield accurate results already. It is hoped that by parameterizing the eddy viscosity calculated for a number of runs, a model for the eddy viscosity can be obtained that extrapolates to drift-wave problems for a larger range of parameters.

The sample simulation mentioned in Sec. 5.2 was used to calculate the eddy viscosity for a simulation with half of its resolution. The resulting eddy viscosity $\nu_{\mathrm{eddy}}(\mathbf{k})$ is plotted in Fig. 6.1 with the linear drive and damping for lines of modes out to the cutoff wave number in two directions in $k$ space. As noted in Sec. 5.2, inertial-range behavior should not be expected in simulations of this kind of plasma turbulence, and there is no inverse cascade of energy from very short wavelengths. While there is a small negative eddy viscosity at long wavelengths for this simulation, it is dynamically insignificant compared to the linear drive and dissipation at long wavelengths. The dominant effect of the eddy viscosity lies in a narrow region near the cutoff where it becomes positive and large compared to the linear drive. The mechanism for this

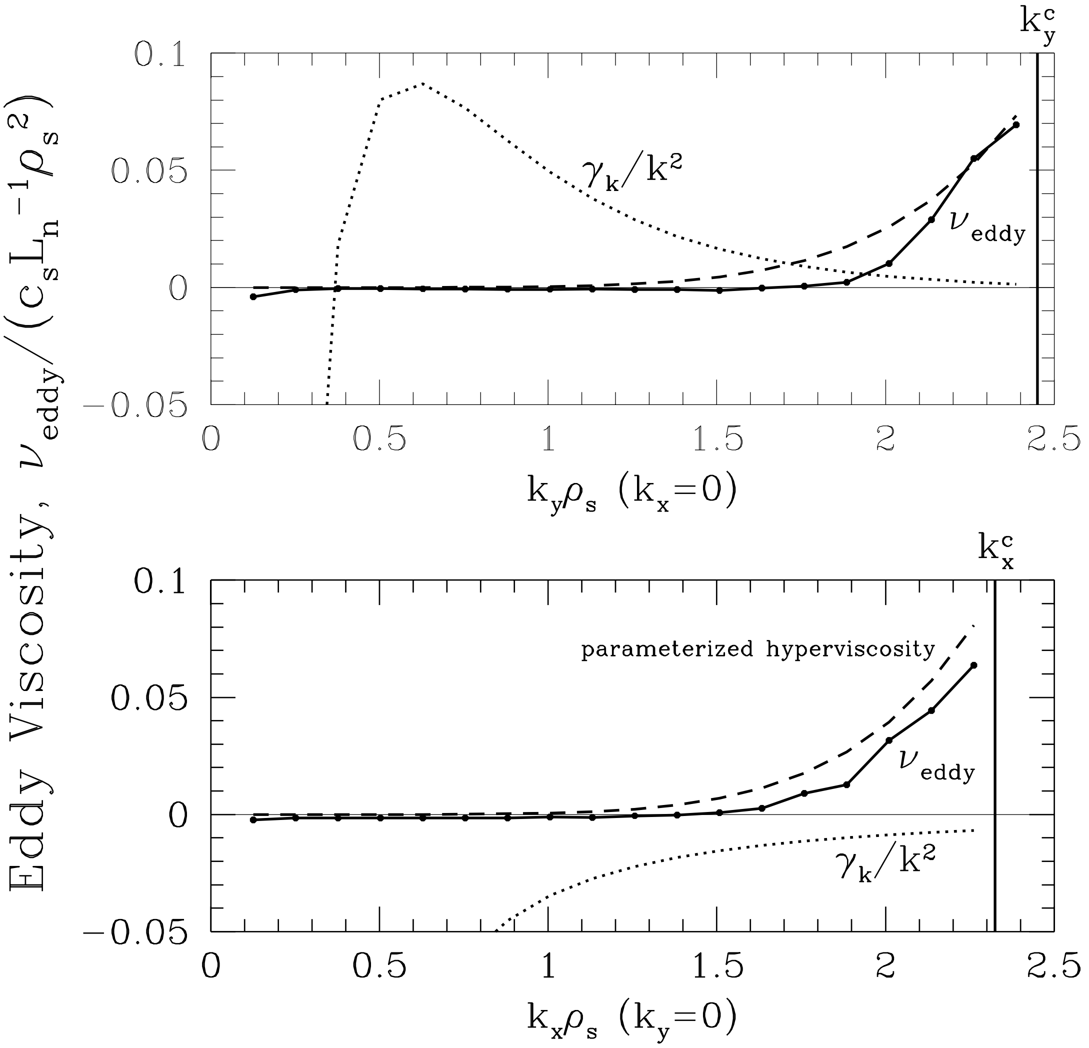


Figure 6.1: Eddy viscosity calculated for the simulation of Fig. 5.2. The transfer was calculated for a box of $37 \times 39$ modes (representing a simulation with half the actual resolution) to modes outside the box, but resolved by the simulation. The dotted line is the linear growth rate, expressed as a viscosity by dividing by $k^2$. The eddy viscosity has a small negative component as $k \to 0$, but it is negligible compared to the linear driving term. The eddy viscosity becomes important in a small region near the cutoff. The dashed line is the parameterized hyperviscosity derived in Sec. (6.2). For these parameters and cutoff wave number, the parameterization provides a good fit to the actual eddy viscosity.

damping near the cutoff is the loss of fluctuation energy from resolved modes by the coherent straining due to long-wavelength modes (Kraichnan 1976). This damping mechanism is probably the dominant physical effect of subgrid modes in drift-wave turbulence simulations, so the focus of this study is to effectively model the positive eddy viscosity in the region near the cutoff.

### 6.1.4 Heuristic Scaling of the Eddy Damping Rate

Consider a fictitious wave packet of short-wavelength fluctuations, localized in $k$ space and real space so that the long-wavelength advecting velocity field looks locally like a shear flow. Without loss of generality, consider the action of the local shear flow, $\mathbf{V}_{\mathbf{E}\times\mathbf{B}}(x, y) = -\theta^{-1} y\widehat{\mathbf{x}}$, where the shearing time is denoted by $\theta$. The advection part of the continuity equation then has the form of a shear flow in Fourier space as well,

$$\frac{\partial}{\partial t}\widetilde{n}_i(\mathbf{k}) + \theta^{-1}\frac{\partial}{\partial k_y} k_x \widetilde{n}_i(\mathbf{k}). \tag{6.14}$$

Fig. 6.2 illustrates this process. The wave packet will be advected in $k$ space in a particular direction depending on the local shear. The random variations of the local shear will thus lead to a random-walk diffusion of this wave packet in $k$ space, with a net transfer of fluctuation energy to high $k$ (Leith 1968).

In the numerical simulation, however, the absence of the nonlinear interactions with unresolved modes and the conservative nature of the nonlinearity cause the cutoff in $k$ space to act as a reflecting boundary. Thus, in Fig. 6.2 the wave packet, represented by the dark circle, would be reflected back to long wavelengths instead of leaving the system. A reasonable estimate of the amount of eddy damping required by an eddy viscosity, therefore, would be given by the inverse of the time that a wave-packet spends in the near-cutoff region of width $\Delta k_{\text{eddy}}$ where the eddy viscosity operates. (In reality a wave packet may enter and leave this region of $k$ space several times as it random walks to the dissipation range, so the eddy viscosity may be reduced from this estimate.) For this example, the velocity of the packet in $k$ space is $\theta^{-1}k_x$ so the time it spends in the edge region is $\theta {k_x}^{-1}\Delta k_{\text{eddy}}$. An eddy-damping rate of the form

$$\gamma_{\text{eddy}}(k) \sim -\theta^{-1} k_c {\Delta k_{\text{eddy}}}^{-1} f\left(\frac{k_c - k}{\Delta k_{\text{eddy}}}\right) \tag{6.15}$$

would therefore effectively damp fluctuations being sheared to high wave number. The maximum damping rate given by the theoretical enstrophy-range eddy viscosity defined in Eq. (6.10) scales as $\nu_{\text{eddy}}(k_c){k_c}^2 \approx \theta^{-1}k_c {k_0}^{-1}$ while $-\gamma_{\text{eddy}}(k_c){k_c}^2 \sim \theta^{-1}k_c{\Delta k_{\text{eddy}}}^{-1}$, so the same basic scaling is obtained if $k_0$ is identified with $\Delta k_{\text{eddy}}$.

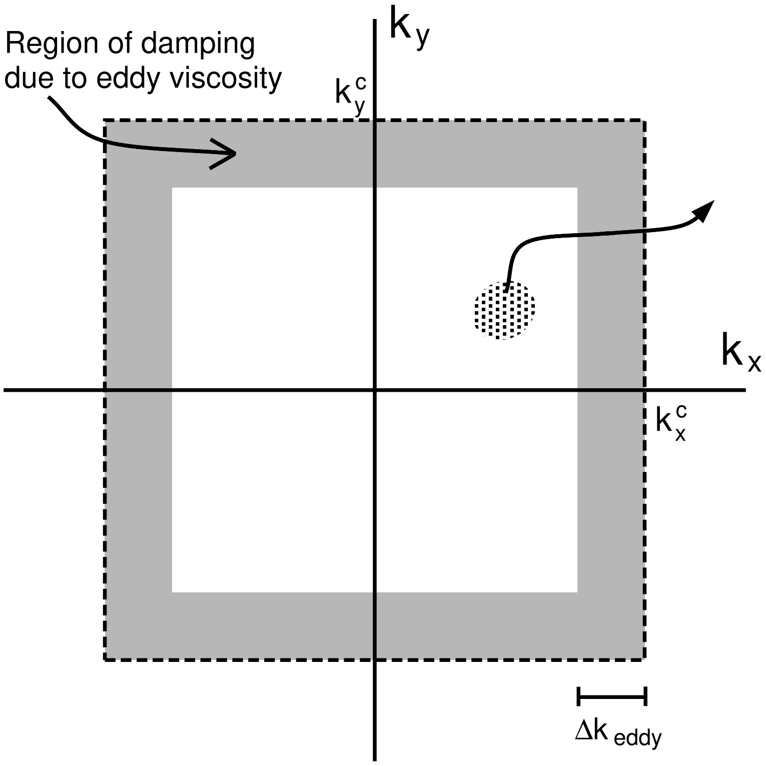


Figure 6.2: Heuristic picture of a fluctuation wave packet undergoing shear. As discussed in Sec. (6.1.4), the region of significant eddy viscosity near the cutoff (the grey region), acts as an absorbing buffer for fluctuation energy that would leave the system unaided if the system were truly unbounded.

### 6.1.5 Hyperviscosity

Hyperviscosity is defined as a damping term of the form

$$\gamma^d_{\mathbf{k}} = -\nu_h(|\mathbf{k}|/k_c)^p, \tag{6.16}$$

where $p$ is larger than two. Hyperviscosity has been used as a numerical tool for simulating high-Reynolds-number turbulence in order to provide an artificially narrow dissipation range in the resolved modes, effectively increasing the extent of the inertial range simulated for a given resolution (Borue and Orszag 1995). Hyperviscosity has been regarded as an artificial damping term that does not attempt to estimate the subgrid interaction. Authors have, however, viewed hyperviscosity as a kind of subgrid model in the way that it serves as a sink for small-scale fluctuation energy (Basdevant and Sadourny 1983).

The choice of power $p$ and size of the hyperviscosity $\nu_h$ is rarely discussed in the literature. Typically the size of the damping is set experimentally so that a dissipation range appears within the resolved modes. Studies of 2D Navier–Stokes turbulence (Basdevant and Sadourny 1983) have found that large powers ($p \sim 16$) work well, but that the optimal choice depends on the resolution of the simulation. With insufficient damping at the cutoff, fluctuation energy will tend towards equipartition in the Fourier modes leading to a spectrum $\Omega(k) \propto k$ towards the cutoff, which disagrees with the converged dissipative result. If the power used is too small, then damping that is sufficient to prevent unphysical behavior at the cutoff will introduce significant damping at long wavelengths and strongly affect the results. On the other hand, there must clearly be an upper limit to the power used. For a very high power there would be virtually no damping for almost all the modes except for a few modes near the cutoff that would be extremely damped. The results would be similar to performing a simulation with those modes removed and no damping on the remaining modes. This behavior may be considered analogous to impedance matching at the end of an electrical cable, where strong reflections occur if the load impedance is either too small or too large.

The constant $\nu_h$ is typically chosen so that modes near the cutoff experience damping that is large compared to the eddy turnover rate. An artificial dissipation region is introduced into the resolved modes that is much narrower in $k$ space than the dissipation region given by the usual $k^2$ damping term. If the precise form of the dissipation does not affect the large-scale dynamics, then the use of artificial damping terms like hyperviscosity can yield significant savings in computation by greatly reducing the required resolution.

## 6.2 Hyperviscosity as a Model for Eddy Viscosity

The exact form of the eddy damping depends on the detailed nature of the saturated spectrum and the mode-mode coupling to unresolved modes. If one could accurately predict the eddy viscosity from theory, then there would be no point in performing numerical simulations. There are a large number of models for drift-wave turbulence, each of which will saturate with a different spectrum, so in general one should expect a different eddy viscosity from that predicted for Navier–Stokes turbulence by Kraichnan (Kraichnan 1976). Hence we are motivated to parameterize the basic features of the eddy viscosity in terms of the large-scale flow.

Hyperviscosity provides significant damping in a narrow region near the cutoff wave number, just as the calculated eddy damping for this model does (Fig. 6.1). An obvious method of fixing the two hyperviscosity parameters, the power $p$ and magnitude $M$ in Eq. (6.19), is to match the width and overall damping rate with the calculated eddy-damping term. The width and the damping are functions of the large-scale flow, so to apply the results to simulations, quantities corresponding to the long-wavelength scale $k_0$ and eddy circulation time $\theta$ must be defined. A surrogate for the long-wavelength eddy turnover time is the volume-averaged shearing rate

$$S(t) = \left[ \frac{1}{L_x L_y} \int_0^{L_x} \int_0^{L_y} S(x,y,t)^2 \, dy \, dx \right]^{1/2}. \tag{6.17}$$

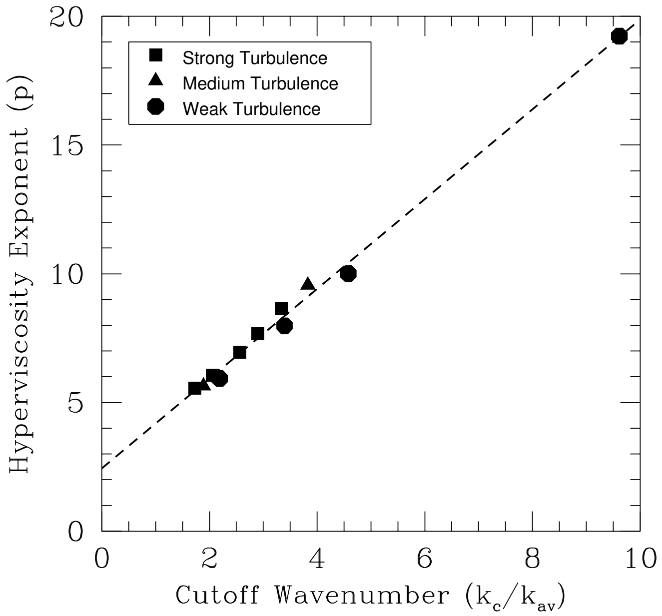


Figure 6.3: Hyperviscosity power predicted from direct numerical simulations.

An average wave number of the large scales is given by dividing the rate of shear by the root mean square of the velocity field,

$$k_{\mathrm{av}} = S\left(\frac{1}{L_x L_y}\int_0^{L_x}\int_0^{L_y} {V_x}^2 + {V_y}^2 \, dy \, dx\right)^{-1/2}. \tag{6.18}$$

We will use the average wave number $k_{\mathrm{av}}$ as an estimate for the long-wavelength scale $k_0$ and the inverse rate of shear $S(t)^{-1}$ as an estimate for the eddy circulation time $\theta$.

The hyperviscosity used for the simulations considered here introduces a damping term of the form

$$\gamma_h = -M\left[\left(\frac{k_x}{k_{xc}}\right)^p + \left(\frac{k_y}{k_{yc}}\right)^p\right] \tag{6.19}$$

into the model, Eq. (5.10), by setting $\gamma_{\mathbf{k}}^d = \gamma_h$. This hyperviscous damping term $\gamma_h$ can be compared to the damping rate $\nu_{\mathrm{eddy}}(\mathbf{k})k^2$ given by the theoretical eddy viscosity of Eq. (6.10), and to the heuristic eddy damping rate defined in Eq. (6.15). The width of the theoretical eddy viscosity scales with the long-wavelength scale $k_0$ while the width of this hyperviscosity scales as $k_c/p$, so the power should scale as $p \propto k_c/k_{\mathrm{av}}$.

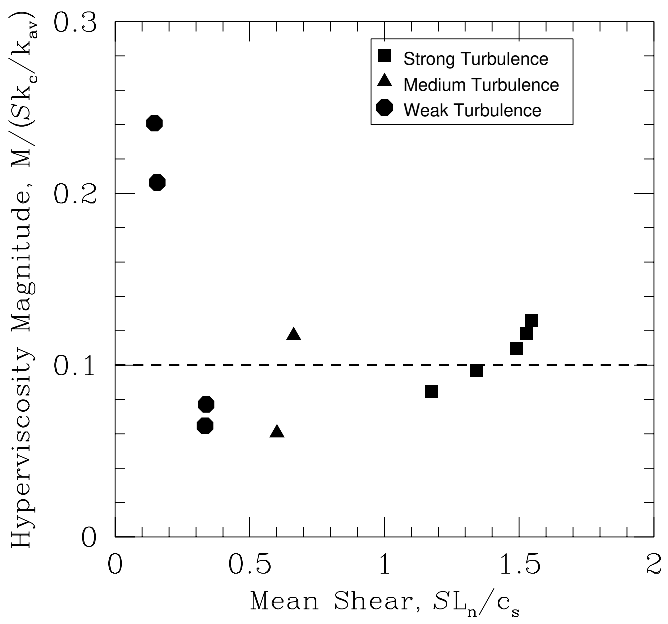


Figure 6.4: Hyperviscosity magnitude predicted from direct numerical simulation.

Comparing the magnitude of the three damping rates at the cutoff wave number $k_c$ gives the scaling for the magnitude, $M \propto Sk_c/k_{\rm av}$.

An estimate for the power $p$ and magnitude $M$ was obtained from the numerically calculated eddy viscosity by setting two moments in $k$ space to zero by

$$\begin{aligned} 0 &= \sum_{\mathbf{k}} \left[ -\nu_{\rm eddy}(\mathbf{k}) k^2 - \gamma_h \right], \\ 0 &= \sum_{\mathbf{k}} \left[ -\nu_{\rm eddy}(\mathbf{k}) k^2 - \gamma_h \right] \min(k_{xc} - |k_x|, k_{yc} - |k_y|). \end{aligned} \tag{6.20}$$

This estimate matches the width and magnitude of the damping region given by the hyperviscosity to that of the eddy viscosity. The estimates for the power and magnitude from simulations with a range of parameters and resolutions are summarized in Figures 6.3 and 6.4. The scaling of the power (and hence the width of the damping region), seems very robust. The estimate from these simulations gives

$$\begin{aligned} p &\sim 1.7 k_c/k_{\rm av} + 2.4, \\ M &\sim 0.1 S k_c/k_{\rm av}. \end{aligned} \tag{6.21}$$

The scaling of the magnitude (Fig. 6.4) is less robust than the scaling of the power (Fig. 6.3). There may be other macroscopic quantities that can be used to refine the estimate for the size of the damping.

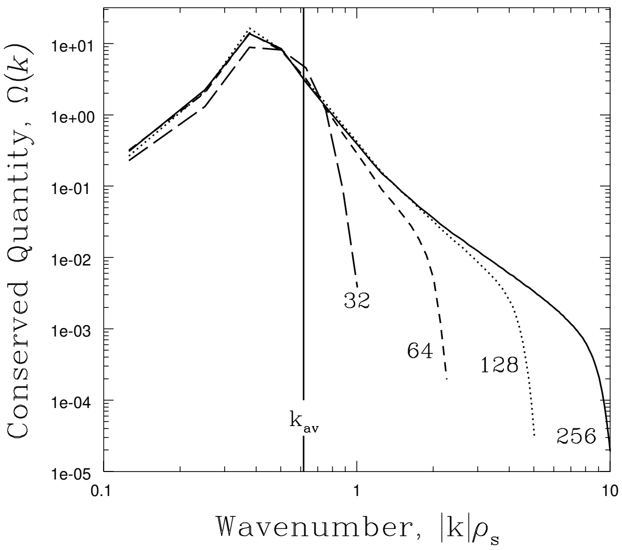


Figure 6.5: Convergence of simulations using hyperviscosity at moderate turbulence levels. (The parameters $\delta_0 = 0.15$, $\alpha = 0.015$, and $\mu = 0.0001$ were used with periodic box size $50\rho_s \times 50\rho_s$.) A hyperviscosity with an *a priori* fixed power $p = 16$ was used as is typically done in simulations of isotropic turbulence. The damping was set to the rate of shear ($\nu_h = S$) to insure that resolved high-$k$ modes were sufficiently damped. The large-scale average wave number $k_{\rm av}$ calculated from the highest-resolution simulation is included for reference.

Note in Fig. 6.4 that the largest variation in estimates for the magnitude of the hyperviscosity (hence the overall eddy damping rate) occurs for low mean shear. In the weak-turbulence regime, the effects of wave dispersion are comparable to or larger than those from the nonlinear mode coupling. The magnitude scaling proposed here is based on the nature of 2D neutral-fluid turbulence where there is no wave physics. Some measure of the wave dispersion could prove useful in improving the parameterization. (On the other hand, it will be shown in the next section that the dissipation model has less impact on the accuracy of simulations in the weak-turbulence regime.)

## 6.3 Tests of Damping Models

Simulations were performed for a range of parameters, and grid sizes ranging from $32 \times 32$ to $256 \times 256$ to test the performance of three dissipation models against each other and against the use of no dissipation model. An ordinary hyperviscosity was

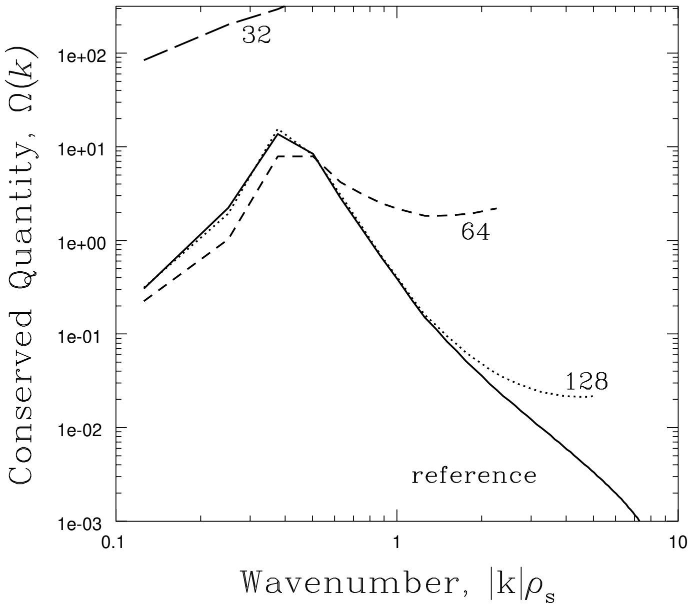


Figure 6.6: Convergence of simulations using no added dissipative terms for the same choice of parameters used in Fig. 6.5. The lower-resolution results failed to give reasonable results in this case.

tested with power $p = 16$ and coefficient set based on the rate of shear, $\nu_h = S$. The Smagorinsky eddy viscosity was tested with the constant $C_s = 0.1$ chosen arbitrarily. Based on the results from the previous section, the parameterized hyperviscosity was tested with power $p = 1.7k_c/k_{\rm av} + 2.4$ and magnitude $M = 0.1S(t)k_c/k_{\rm av}$.

Typically simulations of isotropic turbulence will use an *a priori* fixed-power hyperviscosity to provide the necessary damping. Resulting spectra for simulations using the fixed-power hyperviscosity are shown in Fig. 6.5 for the parameter choice that gave moderate levels of turbulence. The rate of transfer of fluctuations to short wavelengths scales with the rate of shear $S$, so the choice of a hyperviscous damping of the form $S(k/k_c)^p$ corresponds to setting the dissipation wave number to a fixed fraction of the cutoff wave number $k_c$. (The dissipation wave number is the scale at which the damping of the conserved quantity becomes dynamically significant.) The spectrum at long wavelengths observed in simulations (Borue 1993) is a slowly changing function of Reynolds number for the 2D Navier–Stokes enstrophy cascade where hyperviscosity is the primary source of dissipation. Since the physics of this drift-wave model is dominated by production and dissipation of fluctuations at long wavelengths (see Fig. 5.5), there should be an even weaker dependence of the

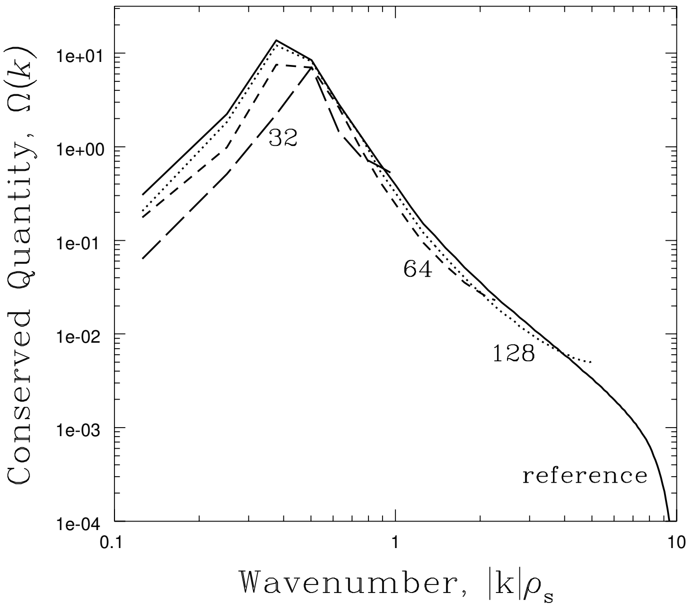


Figure 6.7: Convergence of simulations using the Smagorinsky eddy viscosity with $C_s = 0.1$, for the same choice of parameters used in Fig. 6.5.

long-wavelength saturation on the precise details of the dissipation range. Moving the hyperviscous dissipation scale with the cutoff allows us to resolve more of the small-scale dynamics with increased resolution. The spectra are almost identical at long wavelengths for grid sizes $128 \times 128$ and $256 \times 256$, so we are confident that the $256 \times 256$ case well represents the converged solution.

The results of simulations using no eddy viscosity or hyperviscosity term are shown in Fig. 6.6 for comparison. It is well known that lack of an eddy viscosity leads to unphysical results in Navier–Stokes turbulence when the small-scale dissipation wave number exceeds the cutoff. One might think that since dissipation from terms that model Landau damping at long wavelengths is the dominant drain of energy, then the transfer to small spatial scales can be completely ignored. From the results, this hypothesis is clearly only partially true. Given sufficient resolution, the spectrum converges to the reference spectrum obtained from the highest-resolution hyperviscosity run. The lower resolution runs, however, give wildly inaccurate results despite the fact that the lowest resolution considered here ($32 \times 32$) resolves the primary production and dissipation wave numbers in Fig. 5.5. Drift-wave turbulence will typically exhibit only a moderate separation of scales between the spectral peak and the dissipative range, so it is practical to perform 2D simulations with sufficient resolution

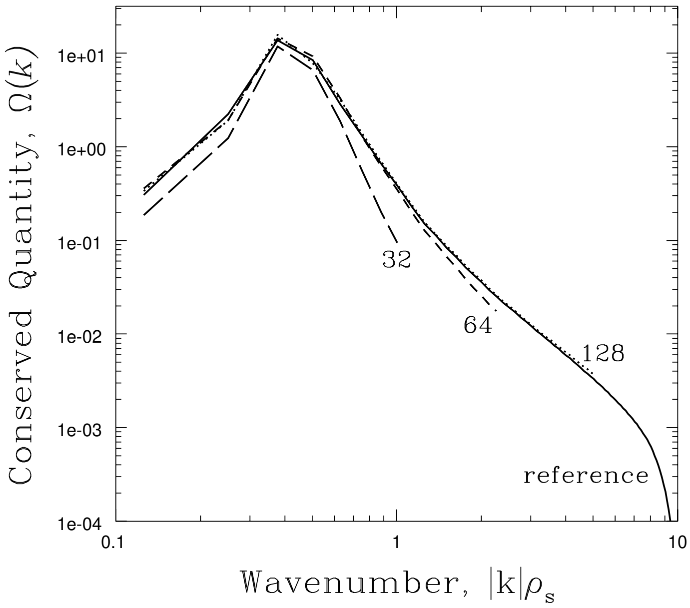


Figure 6.8: Convergence of simulations using the parameterized hyperviscosity ($p = 1.7k_c/k_{\rm av} + 2.4$, $M = 0.1Sk_c/k_{\rm av}$) for the same choice of parameters used in Fig. 6.5.

that an eddy viscosity or hyperviscosity term is unnecessary. On the other hand, for 3D simulations of drift-wave turbulence, the reduction in required resolution can be significant.

Performance of the Smagorinsky eddy viscosity with constant $C_s = 0.1$ for the same parameter choice is shown in Fig. 6.7. Again, given sufficient resolution, the spectrum converges to the reference spectrum. Results at long wavelengths ($k\rho_s \sim 0.4$) for lower-resolution runs are better than those obtained using no additional dissipation terms but not as good as those obtained using a hyperviscosity. Choosing a larger value of the constant $C_s$ will improve the results somewhat at lower resolution but degrades the results for the $128 \times 128$ case. The constant $C_s$ is probably not universal for the kind of turbulence studied here, in contrast to the case of the inertial range in Navier–Stokes turbulence. A fundamental problem with applying any eddy viscosity that gives damping scaling as $k^2$, however, is that providing sufficient damping for modes near the cutoff forces one to introduce a significant artificial damping into the long-wavelength modes that dominate the nonlinear physics.

Simulation results using the parameterized hyperviscosity are shown in Fig. 6.8. In this case, results at low resolution are obtained that are superior to those from all

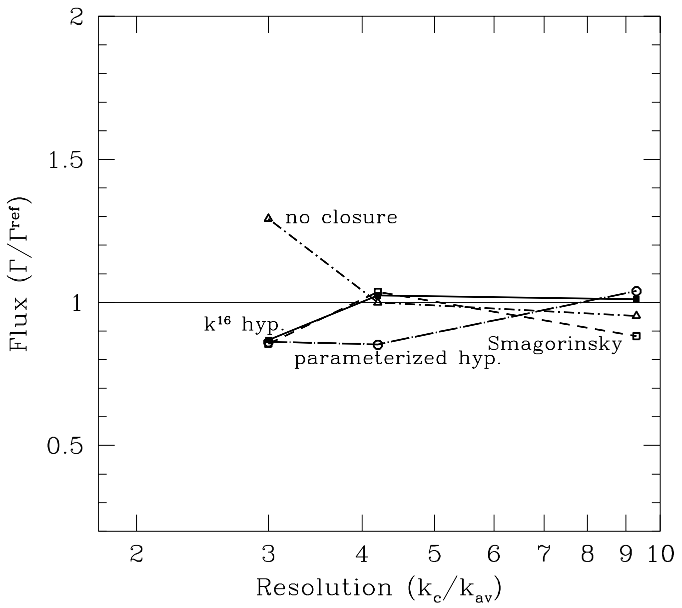


Figure 6.9: Convergence of the measured flux as a function of resolution for the case of weakly driven turbulence. (The parameters $\delta_0 = 0.20$, $\alpha = 0.03$, and $\mu = 0.0001$ were used with periodic box size $40\rho_s \times 40\rho_s$.) The flux is normalized to the flux measured by a reference simulation where $k_c/k_{\rm av} \approx 13$. In this case the nonlinear transfer to shorter wavelengths is a small effect, so the use of a subgrid damping term is unnecessary.

other approaches considered in this study. The performance of the parameterized hyperviscosity indicates that it provides a reasonable model of the actual eddy-damping process. Note that in the lowest-resolution run here a significant portion of driven modes lies beyond the cutoff wave number, so the spectrum falls below the reference spectrum. It is possible that even better results may be obtained for low-resolution simulations by modeling the transfer of energy from unresolved small scales to resolved long wavelengths by adding a negative term to the eddy viscosity to model this backscatter.

To summarize the convergence properties with various dissipation models, we need to define a measure of the resolution. The cutoff wavenumber $k_c$ is a natural measure of the simulation resolution, but there are several choices of wavenumbers that the cutoff can be normalized to. The long-wavelength scale $k_{\rm av}$ defined in this study is a natural choice, which gives $k_c/k_{\rm av}$ as a measure of resolution. This definition seems unnatural to those used to dealing with fluid turbulence simulations. One could argue that the cutoff wavenumber should be normalized to some dissipation wavenumber.

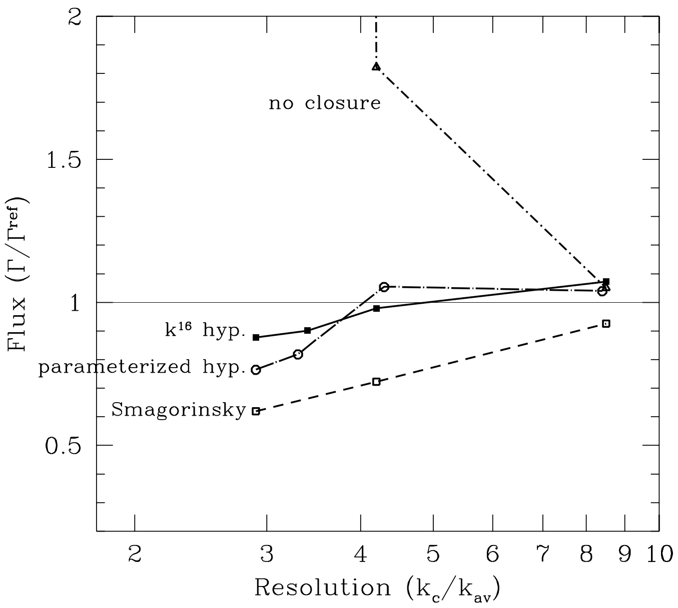


Figure 6.10: Convergence of the measured flux as a function of resolution for the cases of moderately driven turbulence. (See Fig. 6.5 for the parameters.) The flux is normalized to the flux measured by a reference simulation where $k_c/k_{\mathrm{av}} \approx 15$. In this case the nonlinear transfer is sufficiently strong that the simulations will blow up with no damping term for lower-resolution runs. A hyperviscosity with large exponent outperforms the Smagorinsky viscosity.

For these simulations, the bulk of the dissipation occurs at long wavelengths, so a dissipation wavenumber defined for the Landau damping term would be $\sim k_{\mathrm{av}}$. One could define a dissipation wavenumber in terms of the hyperviscous dissipation only. With the parameterized hyperviscosity, however, this dissipation wavenumber is forced to lie near the cutoff wavenumber. For lack of a better definition of resolution, we therefore use the quantity $k_c/k_{\mathrm{av}}$, which can be viewed as a kind of 'Reynolds' number for the inertial range part of the simulation. The true solution can be viewed as the infinite 'Reynolds' number limit. Since the dynamics of the turbulence in these simulations seems to be dominated by the long wavelength production and dissipation, we expect the results to be insensitive to any measure of the scale range of the short-wavelength 'inertial range'.

Convergence of the measured flux is summarized for simulations of weakly driven, moderately driven, and strongly driven turbulence (Figures 6.9, 6.10, and 6.11 respectively). In each case, the measured flux is normalized to a reference value obtained

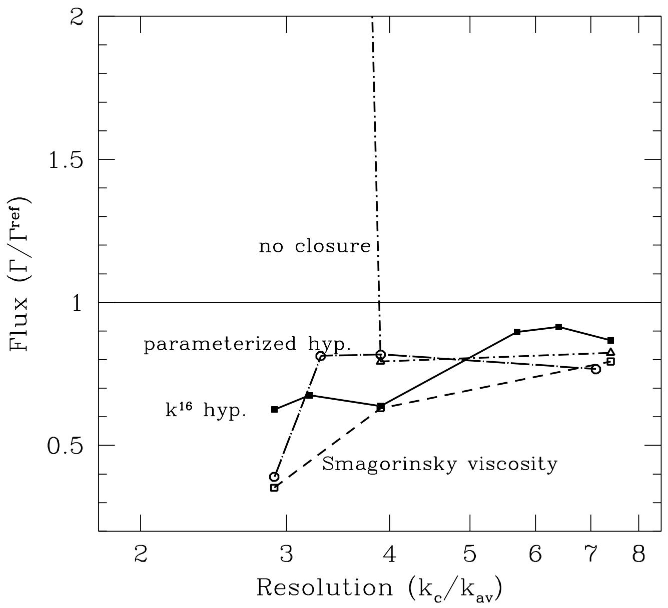


Figure 6.11: Convergence of the measured flux as a function of resolution for the cases of strongly driven turbulence. (See Fig. 5.2 for the parameters.) The flux is normalized to the flux measured by a reference simulation where $k_c/k_{\rm av} \approx 13$. The results are similar to those obtained for the case of moderately driven turbulence (Fig. 6.10).

from a high-resolution (grid size $256 \times 256$) simulation using hyperviscosity. In all cases, the most reasonable results obtained at lower resolution were obtained using the parameterized hyperviscosity or the $k^{16}$ hyperviscosity. For the moderate- and strong-turbulence cases, one obtains reasonable results at resolutions at least a factor of 2 smaller than those necessary for simulations with no added dissipation. For the case of weakly driven turbulence, however, the nonlinear coupling to unresolved modes is less important and there is little difference between any of the models used. In summary, a hyperviscous damping term works effectively in drift-wave simulations at low resolutions (working down to $k_c/k_{\rm av} \sim 4$) and moderate to strong levels of turbulence.

## 6.4 Resolution Requirements

The simulations performed in this study indicate that if the cutoff wave number is at least a factor of 3 or so greater than the long-wavelength scale $k_{\rm av}$ (or roughly a factor of 6 larger than the spectral-peak wave number), then reasonable results can

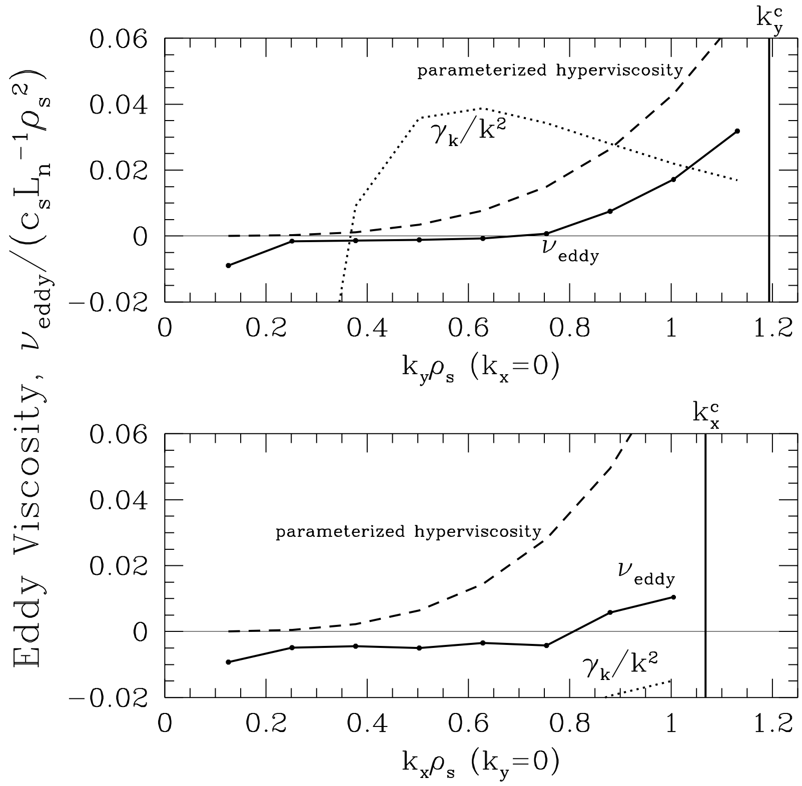


Figure 6.12: Eddy viscosity calculated for a low-resolution simulation at moderate turbulence levels of turbulence. (See Fig. 6.5 for the parameters.) In this case, the parameterized hyperviscosity grossly overestimates the damping. Note that the calculated eddy viscosity is anisotropic in this case and has a significant negative component at long wavelengths. Simulations at this resolution estimated $k_c/k_{\rm av} \approx 3$.

be obtained with the use of a hyperviscosity. There are several sources of error in calculating macroscopic quantities such as the flux from lower-resolution simulations. Contributions to the flux from unresolved modes may be significant or the resolved modes may fail to saturate at the correct level. Incorrect saturation levels may be due to the failure of our parameterization to model the eddy viscosity or from the failure of eddy viscosity to model the physics of unresolved modes.

For the lowest resolution simulations considered in this study, the contribution to the flux from unresolved modes is too small (5% or less) to explain the discrepancy between the calculated flux at low and high resolution. As is clear from the spectra in Figures 6.5 and 6.8, the error in the calculated flux at the lowest resolution comes from the failure of resolved modes to saturate at the correct level. The eddy viscosity calculated for grid size $32 \times 32$ for moderate levels of turbulence is plotted in Fig. 6.12. The parameterization overestimates the eddy viscosity significantly in

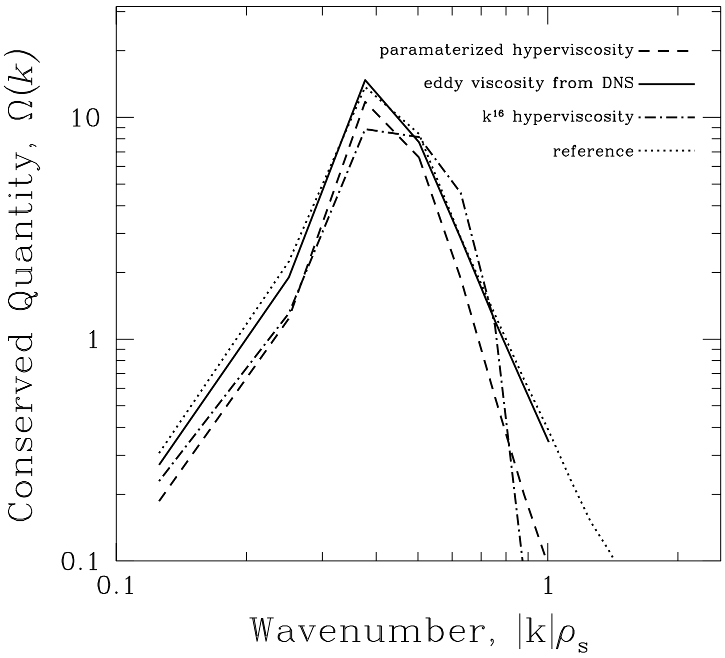


Figure 6.13: Comparison of simulations at low resolution using hyperviscosity and the calculated eddy viscosity in Fig. 6.12. (At this resolution, the Smagorinsky eddy viscosity gives very poor results, and simulations with no added dissipative term blow up.)

this case. As well, the calculated eddy viscosity is significantly anisotropic and the negative viscosity at long wavelengths is of size comparable to the positive portion that the parameterization models. For comparison, the calculated eddy viscosity was used in a simulation at this resolution. The resulting spectrum is shown compared to the hyperviscosity simulations and the high-resolution reference spectrum in Fig. 6.13. Using the calculated eddy viscosity gives very accurate results in this case. The flux calculated from this simulation is within 5% of the flux calculated from the highest-resolution run.

The current limits of the parameterized hyperviscosity are therefore clearly due to its failure to model accurately the eddy viscosity at low resolution. Future work will attempt to improve the parameterization of the magnitude of the hyperviscosity, generalize the parameterization to provide anisotropic damping, and possibly to incorporate a model for the negative viscosity at long wavelengths. Also, it may be useful to examine the effects of wave dispersion on the eddy viscosity. It is not clear from this work which of these improvements will have the greatest effect on improving the accuracy of low-resolution simulations.

## 6.5 Summary

A new parameterized hyperviscosity, Eqs. (6.19) and (6.21), was derived by analyzing the eddy viscosity calculated from simulations with a range of parameters and resolutions. Simulations using the parameterized hyperviscosity perform somewhat better than those using hyperviscosity with fixed power, and significantly better than those using no extra damping term or a Smagorinsky-type eddy viscosity. Accurate results are obtained provided the cutoff wave number, $k_c$, is approximately four or more times greater than the characteristic wave number $k_{\mathrm{av}}$ of the advecting velocity. At lower resolutions, the parameterization fails to accurately model the eddy viscosity.

Because this hyperviscosity is based on physics generic to most drift-wave turbulence, application to more complete models is straightforward. This hyperviscosity is very useful computationally, since reducing resolution requirements by even a factor of 2 reduces the computational requirements by a factor of 8 in two dimensions, or 16 in three dimensions.